An empirical comparison among aftershock decay models

Paolo Gasperini, Barbara Lolli

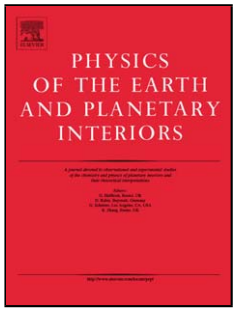

Title: An empirical comparison among aftershock decay models

Authors: Paolo Gasperini, Barbara Lolli

PII: S0031-9201(09)00064-8
DOI: doi:10.1016/j.pepi.2009.03.011
Reference: PEPI 5158

To appear in: *Physics of the Earth and Planetary Interiors*

Received date: 8-8-2008
Revised date: 13-3-2009
Accepted date: 15-3-2009

Please cite this article as: Gasperini, P., Lolli, B., An empirical comparison among aftershock decay models, *Physics of the Earth and Planetary Interiors* (2008), doi:10.1016/j.pepi.2009.03.011

An empirical comparison among aftershock decay models

Paolo Gasperini and Barbara Lolli

Dipartimento di Fisica

Università di Bologna

Viale Berti-Pichat 8

I-40127 Bologna (Italy),

e-mail: paolo.gasperini@unibo.it, barbara.lolli@unibo.it

Abstract

We compare the ability of three aftershock decay models proposed in the literature to reproduce the behavior of 24 real aftershock sequences of Southern California and Italy. In particular, we consider the Modified Omori Model (MOM), the Modified Stretched Exponential model (MSE) and the band Limited Power Law (LPL). We show that, if the background rate is modeled properly, the MSE or the LPL reproduce the aftershock rate decay generally better than the MOM and are preferable, on the basis of the Akaike and Bayesian information criteria, for about one half of the sequences. In particular the LPL, which is usually preferable with respect to the MSE and fits well the data of most sequences, might represent a valid alternative to the MOM in real-time forecasts of aftershock probabilities. We also show that the LPL generally fits the data better than a purely empirical formula equivalent to the aftershock rate equation predicted by the rate- and state-

dependent friction model. This indicates that the emergence of a negative exponential decay at long times is a general property of many aftershock sequences but also that the process of aftershock generation is not fully described by current physical models.

Introduction

The most commonly used formula to reproduce the decay of aftershock rate after a mainshock, also adopted in procedures for the real-time forecast of aftershock probabilities in California (Gerstenberger et al., 2007), is the Modified Omori Model (MOM, Utsu, 1961)

$$\lambda_{MOM}(t) = \frac{K}{(t+c)^{p}} \qquad [1]$$

where $\lambda_{MOM}(t)$ is the intensity (the rate) of a non stationary Poisson process, and p, c and K are free parameters. The MOM is empirical in nature but it was found to be compatible with the rate- and state-dependent friction model proposed by Dieterich (1994).

A characteristic of the MOM is to predict an infinite number of possible future aftershocks (that is an infinite number of potential faults) if the power law exponent p is lower than or equal to 1. Since such p values are often observed for real sequences, the MOM might appear physically unrealistic. Few alternative formulations, proposed in the last decades, overcome this limitation of the MOM. We mainly consider here two of them: the Modified Stretched Exponential Model (MSE, Kisslinger, 1993; Gross and Kisslinger, 1994) and the Band Limited Power Law (LPL, Narteau et al., 2002; 2003). Both MSE and LPL assume that a negative exponential decay emerges at long times, hence they predict a finite number of aftershocks (and faults), independently of the value of the power law exponent. The intensity of the MSE can be written as

$$\lambda_{MSE}(t) = (1-r)N^{*}(0)\left(\frac{d}{t_0}\right)^{1-r}\frac{(t+d)^{r}}{t_0^{1-r}}\exp\left(\frac{t+d}{t_0}\right)^{1-r} \qquad [2]$$

where $N^{*}(0)$ is the total number of potential shocks at the time of the mainshock (t=0), t_0 is the relaxation time of the negative exponential decay process, d a delay time (corresponding to parameter c of the MOM) and $0<r\leq 1$ the power-law exponent.

The intensity of the LPL is given by

$$\lambda_{LPL}(t) = B\frac{\Gamma(q,\ t/b) - \Gamma(q,\ t/a)}{t^{q}} \qquad [3]$$

where q is the power-law exponent, B is a normalizing constant (similar to K of the MOM), $_a > _b$ are two parameters (having the physical dimensions of rates) that controls the behavior at long and short times respectively, and γ indicates the incomplete Gamma function

$$q,x \quad \int_0^x z^{q\ 1} e^{\ z} dz \qquad [4]$$

When $_b \quad _a$ (as it may be assumed usually) the behavior of the LPL can be described as the superposition of three regimes that control the rate at different times: an initial linear decay, which is followed by a power-law and, at large times, by a negative exponential. Narteau et al (2003) suggested to considering two times $t_1 \quad t_2$ that correspond to the transition between the linear and the power-law and between the power-law and the exponential decays respectively. They are defined as the times at which the ratio between aftershock rates predicted by LPL and by a pure power-law is χ. Narteau et al. (2003) report the values assumed by t_1 and t_2, for values of the ratio χ ranging from 0.8 to 0.99 while Lolli et al. (2009) proposed to use $t_b \quad t_1 \, 2^{\ q}$ and $t_a \quad t_2 \, 1/e$ (where e is the base of natural logarithms) as they corresponds approximately to c of the MOM (or d of MSE) and t_0 of the MSE respectively. We will adopt such derived parameters t_b and t_a in the following references to the LPL.

Both MSE and LPL are based on reasonable physical assumptions but Lolli and Gasperini (2006) showed that MSE and LPL are preferable with respect to the MOM for about one fourth of the real aftershock sequences of Southern California and Italy only. They hypothesized that the limited duration of the observing time interval they choose (one year) might penalize the MSE and the LPL with respect to the MOM when the exponential decay emerges later than the end of such interval. In this work we will test such hypothesis by considering a longer observing interval of four years. We also consider here the possibility that the background rate (not modeled by Lolli and Gasperini, 2006) might play a role in assigning the preference to the MOM in some cases. The background seismicity rate is accounted simply by a constant rate μ (to be determined together with the other parameters of the various decay models) added to the rate equations [1] [2] and [3].

Data sources and sequence detection

We use essentially the same datasets analyzed by Lolli and Gasperini (2006) but we extend the analysis to a longer time interval of four years after the mainshock and consider the catalogs of southern California and Italy up to July 2008 and May 2008 respectively (instead of December 2004). For California we use the revised catalog from 1932 to 2008 available from the Southern California Earthquake Center (SCEC) site (http://www.scecdc.scec.org/). For Italy, we merged several catalogs of Italian instrumental earthquakes covering the time interval from 1960 to May 2008. From 1960 to 1980, we used the catalog of the Progetto Finalizzato Geodinamica (Postpischl, 1985) with magnitudes corrected according to Lolli and Gasperini (2003); from 1981 to 1996, we used the *Catalogo Strumentale dei Terremoti Italiani* dal 1981 a 1996 Version 1.1 (CSTI Working Group, 2004); from 1997 to 2002, we used the Catalogo della Sismicità Italiana 1.1 (Castello et al., 2005); finally, from 2003 to 2008, the data are taken from the instrumental bulletin of the *Istituto Nazionale di Geofisica e Vulcanologia* (INGV) available from site http://www.ingv.it/~roma/reti/rms/bollettino. Following Ouillon and Sornette (2005), we assumed the completeness of the southern California catalog for M_L>3.0 in 1932 and later years, for M_L>2.5 in 1975 and later years, M_L>2.0 in 1992 and later years, and M_L>1.5 in 1994 and later years. For Italy we assumed the completeness for M_L>2.5 for 1984 and later (Lolli and Gasperini, 2003), and for M_L>3.0 before 1984.

In a first step we use the same sequence detection algorithm adopted by Lolli and Gasperini (2006) that defines the influence zone of any shock as a circular area centered in the epicenter and assumes as mainshocks (triggering the sequences) all earthquakes with magnitude not lower than 5.0 that are not included in the influence zone of a larger shock. The time window is fixed to four years after the mainshock while the radius R of the influence zone is chosen as a function of magnitude as Log10(R)=0.1238M+0.983 (that closely corresponds to Table 1 of Gardner and Knopoff, 1974).

Only the shocks shallower than 40 km and with magnitude above completeness threshold are included in sequences. To reduce the possible incompleteness in the first times after the mainshock we only consider the aftershocks with magnitude not lower than mainshock magnitude M_m minus 3.5.

As the Gardner and Knopoff (1974) radius is likely to overestimate the size of the mainshock influence zone, in a second step we performed an analysis of correlation between the shock rates observed at different distances from the mainshock during a time interval of 200 days after the mainshock. In particular, for distances r varying from 0 to R, we correlate the sequence of rates observed (over 5 days bins) inside the circle with radius r and inside the circular ring with minimum and maximum radius r and R respectively. For each sequence we assumed as influence distance (reported in Table 1 as R_i) the largest r for which the correlation between the sequences of rates is significant at the 0.05 level.

To grant a reliable determination of model parameters we consider for the analysis only the sequences including 100 shocks at least within the four years time interval following the mainshock. Moreover, since all the simple decay models we consider are not suitable to reproduce complex sequences with strong secondary clustering we excluded from our dataset, by a visual analysis of the plot of the rate over 5 days bins, the sequences showing at later times one or more peaks of the shock rate with amplitude of the same order of magnitude of the peak following the mainshock.

The detected sequences are listed in Table 1. The longer time window (four years instead of one) and the different completeness thresholds and selection criteria here adopted reduces the number of sequences (from 37 to 18 for California and from 10 to 6 for Italy) with respect to those detected by Lolli and Gasperini (2006).

Analysis

We estimated the parameters of each decay model by the maximum likelihood method (Ogata, 1988). To maximize the likelihood we use an algorithm (Lolli et al., 2009) that combines a random search over a reasonable interval of the parameters space and Newton-like optimizations (Dennis and Schnabel, 1983) of the best random solutions. We estimate the parameters of our sequences both with and without the inclusion of the constant background term □ and by considering different lengths of the observing interval of 3, 6, 12, 24 and 48 months.

We compare the goodness-of-fit of the different decay models by three criteria: the corrected Akaike Information Criteria (AIC_c, Akaike, 1974; Hurvich and Tsai, 1989), the corrected Bayesian Information Criteria (*BIC*, Schwartz, 1978; Draper, 1995) and the simple maximum log-likelihood function l_{max}. For the AIC_c and *BIC* we adopt (consistently with Lolli and Gasperini, 2006) the following scores

[5]

[6]

where k is the number of free parameters (3 for the MOM, 4 for MSE and LPL and one more for all models when the background rate □ is considered), and n is the number of data (the number of aftershocks in each sequence). With these formulations, which differ from the usual ones for the sign and for a factor of 2, the best model is the one giving the highest score.

In the following comparisons, we will also consider l_{max} because we might hypothesize that the additional parameter of the MSE and LPL, which models the exponential decay, might not be able improve significantly the fit (and increase correspondingly the log-likelihood function) when the length of the observing time interval (the assumed duration of the sequence) is short with respect to the relaxation time (t_0 for the MSE and about t_a for the LPL). In these cases the penalty terms assigned by AIC_c and *BIC* to the additional parameter might be oversized. Moreover, the model with the highest log-likelihood, whatever the number of parameters, is the one that best reproduce

the behavior of the rate. Hence it is the most suitable for real-time forecast of aftershock probabilities, when the peculiar properties of the active sequence are not known well.

Results and discussion

The parameters of the various models and the relevant goodness-of-fit estimators without and with background are listed in Table 2, for the longest time interval of 48 months (1460 days). For the computations not considering the background rate (Table 2, left), the maximum likelihood estimates of parameter p_3 (corresponding to the exponential decay characteristic time t_0 for the MSE and t_a for the LPL) are in most cases definitely larger than the duration of the observing time interval (highlighted with bold type) and often coincides with the upper limit (Up lim.) of 10^7 days we imposed in likelihood maximization. Conversely, when the background rate is included in computations (Table 2, right), the estimates of p_3 are in most cases shorter than the observing interval (on the order of some weeks to some months). We can also note in Table 2 a general increase of the estimated power law exponent (p1) for all of the models when the background term is considered. For some sequences (*e.g.* cal08, cal11, cal12, cal16) such increase is particularly relevant for the MOM (from about 1 to 1.5 and more). As shown by Gasperini and Lolli (2008) by simulation of synthetic sequences, such high *p* values for the MOM might be the symptom of an early startup of the exponential decay. Parameter p2 (the initial delay time) is not affected instead very much by the inclusion of background. It only tends to slightly increase as a consequence of the increase of the power law exponent, being the two parameters correlated to each other (Gasperini and Lolli, 2006).

The inclusion of the background has also the effect to improve the fit of the three models as shown by the increase of maximum log-likelihoods (l_{max}) for almost all sequences and models. The AIC_c and *BIC* scores are also higher for most sequences. The sequences showing lower AIC_c scores (cal02, cal03, cal06, cal07, cal10, cal17, ita01, ita06) and *BIC* (cal01, cal02, cal03, cal06, cal07,

cal10, cal17, ita01, ita06) for the best model (highlighted with bold type) are characterized by relatively low background rates. In these cases the slight improvement of the likelihood function induced by the additional parameter (the background rate) is not large enough to compensate the penalty terms added by the information criteria.

In the following we will evaluate the relative efficiency of the different models by counting the number of sequences for which each model is the best among the alternatives, according to the three criteria. The results are represented as line plots of such counts as a function of the considered length (of 3, 6, 12, 24 and 48 months) of the time window.

Fig. 1 concerns sequences of Southern California when the background rate is neglected. We note (in Fig. 1a) that the MOM is preferable with respect to the other models according to the AIC_c for more than 2/3 of the sequences. Such prevalence is clearer for *BIC* (Fig. 1b), for which the MOM is preferable with respect to MSE and LPL for more than 3/4 of the sequences. These results are very similar to those obtained by Lolli and Gasperini (2006) on a different set of sequences. We can note that the number of sequences that are better fitted by the MOM increases slightly with the increasing the duration of the time window. Fig. 1c shows that, at the maximum duration of 48 months, the MOM has the highest maximum log-likelihood l_{max} for 7 of the 18 sequences.

In Fig. 2 we report the same computations of Fig. 1 when the background rate is included into the rate equations as an additive constant term μ. It is evident how the MSE and the LPL definitely improve their performances with respect to the MOM. For AIC_c (Fig. 1a), the LPL and the MSE are preferred with respect to the MOM for more than one half of the sequences while for *BIC* (Fig. 1b) the preference goes to MSE or to the LPL for 8 sequences over 18 (Table 3). For the longer time window (48 months), the maximum log-likelihood (Fig. 1c) of the MOM is higher than those of the two alternative models for only one sequence (cal12). We can also note that the numbers of preferences for the various models are weakly dependent on the duration of the observing interval.

A similar behavior was shown by the Italian sequences. Even in this cases the values of p3 decreases while p1 and p2 increases when the background is included in computations (Table 2). In

Fig. 3 we report the number of preferences for the various model only for the AIC_c, which represent an intermediate weighting of the additional parameters between the simple maximum log-likelihood (zero weight) and the *BIC* (highest weight). We can see that the LPL definitely improves its performance with respect to both the MOM and the MSE when the background is considered. For the longer time window of 48 months, only two Italian sequences (ita02, ita03) show larger scores for the MOM.

These evidences indicate that the emergence of exponential decay is a general characteristic of most sequences both in Southern California and Italy and that the background rate (if not appropriately modeled) has the effect to hide such emergence in many cases.

In summary (Table 3), for the longer time window of 48 months the MSE or the LPL perform better than the MOM for 15 sequences over 24 for AIC_c, 11 for *BIC* and 23 for $l_{\max}$, when the background is properly modeled. The MSE and the LPL individually have both a larger $l_{\max}$ than the MOM for 18 sequences over 24 but a larger AIC_c scores for 8 and 14 sequences respectively and larger *BIC* scores for 8 and 10 sequences respectively.

The direct comparison between LPL and MSE shows that the former is preferable with respect to the latter for 16 sequences versus 8 for all of the scores (as the two models have the same number of free parameters). We can also note from Table 2 that for the six sequences (cal03, cal07, cal09, cal12, cal 13 and cal17) for which the MOM has a higher log-likelihood score than the LPL the log-likelihood difference is on the order of a few units at most, indicating that the two models show a very similar fit. Hence, even though the exponential decay, on the basis of information criteria, might be not necessary to reproduce some sequences, we can assert that the LPL represents the most suitable model when the actual properties are not known well, as in real-time forecasting of aftershock probabilities (Gerstenberger et al., 2007) of an active sequence.

Comparing the LPL with the Dieterich (1995) rate equation

To better understand the physical implication of the preference given to the LPL we will attempt an empirical comparison between such model and the rate equation implied by the Dieterich (1994) rate- and state-dependent friction model

$$\lambda(t) = \frac{\mu_r \dot{\tau} / \dot{\tau}_r}{\left[\frac{\dot{\tau}}{\dot{\tau}_r}\exp\left(\frac{-\Delta\tau}{A\sigma}\right) - 1\right]\exp\left[\frac{-t}{t_c}\right] + 1} \quad [7]$$

where $_r$ is the background rate before the mainshock, $\dot{\tau}_r$ and $\dot{\tau}$ are the shear stress rates prior to and following the shear stress step $\square$ induced by the mainshock, A is a fault constitutive parameter, $\square$ the normal stress and $t_c = A\sigma / \dot{\tau}$ a characteristic relaxation time. When the stress after the mainshock is about constant ($\dot{\tau} \approx 0$) eq. [7] becomes equivalent to the Omori's law [1] (with $\square$). For $\dot{\tau} \neq 0$, eq. [7] also gives the Omori's law at short times (t/t_c 1) but merges to the steady state background rate at long times (t/t_c 1).

The formulation of eq. [7] is not particularly suitable to empirically fitting real sequences, because the maximum likelihood method is not able to constrain independently the 6 unknown parameters ($_r$, $\dot{\tau}$, $\dot{\tau}_r$, , A,) from sequence data due to their mutual correlation. Although some assumptions could be made on the values of some parameters we will adopt here a purely empirical approach where the 6 free parameters of eq. [7] are combined into 3

$$\lambda_{DRL}(t) = \frac{\mu}{[C-1]\exp\left[\frac{-t}{t_c}\right] + 1} \quad [8]$$

where $\mu = \mu_r \dot{\tau} / \dot{\tau}_r$ (the steady state background rate after the mainshock), $C = \frac{\dot{\tau}}{\dot{\tau}_r}\exp\left(\frac{-\Delta\tau}{A\sigma}\right)$ and t_c are empirical parameters to be determined by maximum likelihood estimation. For the sake of a comparison with the LPL, t_c has a meaning comparable t_a, and the product Ct_c roughly corresponds (see eq. [16] in Dieterich, 1994) to c of the MOM an then to t_b of the LPL. We must note that such form [8] of the Dieterich rate law (DRL) maximizes the ability to fit the data because it does not imply any physical constraint on the parameter values. So its performance might be

slightly better than those of the original formula (eq. [7]) when a physically consistent value is assigned, for example, to [redacted].

In Table 4 we compare the estimated values of parameters μ, Ct_c (p2) and t_c (p3) as well as the goodness-of-fit scores of the DRL model with the parameters and the scores of the LPL (including background), for the same set of sequences analyzed previously (Table1) and the maximum duration of 48 months. The values of [redacted] as well as of Ct_c with t_b (p2 in Table 4) appear reasonably consistent for most sequences. On the contrary t_c is usually larger than t_a (p3 in Table 4) in most cases.

For all but four sequences (cal03, cal07, cal09, cal17), the maximum log-likelihood l_{max} is larger for the LPL than for the DRL. The AIC_c and BIC scores are slightly less favorable to the LPL, due to the lower number of free parameters of DRL (k=3) with respect to the LPL (k=5 including the background rate). In Fig. 4 we plot the behavior of the number of preferences of AIC_c, BIC and l_{max} scores for the two models as a function of the duration of the time window over which the sequences are observed. For short durations (3 and 6 months) the, LPL appears preferable with respect to the DRL for about 2/3 of the 24 sequences. The preferences for the LPL tend to increase for increasing durations up to 24 months. Then the performance of the LPL worsens slightly and for 48 months (Table 3) the preferences for the LPL and DRL become respectively 17 versus 7 for AIC_c, 15 versus 8 for BIC, and 20 versus 4 for l_{max}.

This behavior can be explained by the interplay between the log-likelihood differences and the penalty terms of the AIC_c and BIC scores: the likelihood difference between the LPL and the DRL tends increase (Fig 4c), for increasing durations from 3 to 12 months, while for larger durations the tendency reverses and even the penalty terms tend to favor more the DRL, due to the increasing number of data.

In summary, the LPL performs generally better than the DRL and is definitely the most suitable model when the aim is to reproduce well the behavior of the aftershock rate. However the DRL,

280 which with only three free parameters shows to explain well a significant portion of the sequences,
281 appears to pick much of the physics of the process of aftershock generation (albeit not all).
282
283 **Visual comparison of rate decay models**
284
285 To better describe the different performance of various models, we plot in Fig. 5 the behavior with
286 the time elapsed after the mainshock of the observed (symbols) and predicted (lines) rates for two
287 sequences (cal16 and ita02) that show the clear emergence of the exponential decay at relatively
288 long times when the background is modeled. We can see how the LPL (blue) and the MSE (green)
289 models, are able to reproduce better than the MOM (red) the transition of the rate to the background
290 level at times on the order of 10^2 days. Moreover they also seem both to describe better than the
291 MOM the rate evolution in the first times after the mainshock (< 0.1 days). In both cases the DRL
292 (black) appears to be too "rigid" to follow well the behavior of aftershock rate decay. It tends to
293 overestimate the rate at short and long times and to underestimate at intermediate times (0.1 to 10
294 days). We can argue that the assumed functional form of the transition to the background rate at
295 long times and the power law exponent fixed to 1 at intermediate times prevent a good fit even at
296 short times.
297 In Fig 6 we report, for the same two sequences, the differences between the observed $N_{observed}(t)$ and
298 predicted $N_{model}(t)$ cumulative number of aftershocks with time. The predicted numbers are
299 computed, for various models, as time integrals of the rate functions from the time t_1 of the first
300 aftershock to the time t_i of each i-th aftershock
301 [9]
302 while the observed cumulative number is simply $N_{observed}(t_i)=i$. These plots confirm that the MOM
303 has generally larger differences than MSE and LPL both at short and long times, while the DRL
304 largely underestimates (positive difference) the cumulative number of shocks at times between few

days and 200 days. For sequence cal16 we can note a marked negative difference for all models at times between 1 and 3 years that rapidly converge to 0 at larger times. This might indicate that the decay of the main sequence is probably slightly faster than that predicted by all of the models but the occurrence of a burst of shock (maybe due a small sequence) at about 3 years after mainshock prevents a more accurate modeling of the behavior at long times. These late shocks do not affect much the fit at times shorter than three years because the maximum likelihood estimation of parameters is controlled by the more numerous shocks occurring in the first part of the sequence.

In Fig. 7 we show the behavior with time of the rate (a) and of the cumulative number difference (b) for a sequence (cal08) characterized by a high power-law exponent (p=1.86 for the MOM and q=1.54 for the LPL), when the background is included in computations. We can see how the MOM (red) and the LPL (blue) curves are almost superimposed among each other. In fact, although the LPL has higher l_{max} and AIC_c, the MOM is preferable according to BIC (see Table 2). Such high value of the power-law exponent prevents a good fit by the MSE (green), for which r is limited in the interval]0,1[and by the DRL (black), which assumes a power law exponent equal to 1. This suggests that Dieterich (1994) model might neglect some unknown physics properties of the aftershock generation process.

Control experiments

As the behavior of aftershock sequences in the first times after the mainshock might not be due to true physical processes but rather to the incompleteness of the seismic catalog (Narteau et al., 2002; Lolli and Gasperini, 2006), we tested the stability of our computations as a function of the starting time of the interval over which the analysis is performed. We rerun our computations, for the longest time interval of 48 months, but removing from the datasets the first 10 minutes (0.007 days), the first hour (0.042 days) or the first day. In the first two cases (Table 5), the results of the comparison between MOM, MSE and LPL are similar to those obtained using the entire sequences.

We can note only a slight increase of the preferences to the MOM with respect to the alternative models MSE and LPL (2 sequences more for AICc and 1 for BIC and l_{max}) and an increase of preferences to LPL with respect to MSE (3 sequences more). The direct comparison between LPL and DRL also gives similar results with a slight increase of preferences to LPL.

When instead the first day is not considered in the analysis, the preferences to the MOM with respect to MSE and LPL increase further by a couple of sequences for l_{max} but more clearly for the other criteria so that about 20 of the 24 sequences give a preferences to the MOM according to AICc and BIC. In this case we also have a dramatic increase of p above 1.5 (up to 4) and of c above 1 day (up to 31 days), for many sequences (Table 6). Such values of MOM parameters are rarely reported in the literature and can be considered unrealistic and not justified physically. In fact, many authors have argued that c should be zero in principle and that non-zero values are due to the incompleteness of the catalog (Narteau et al., 2002; Lolli and Gasperini, 2006) or to physical processes occurring at very short times after the mainshock (Nanjo et al., 2007). When the first part of the sequence is not considered in computations, such incompleteness or such processes cannot influence significantly the estimated parameters, hence the high values of p and c estimated when Ts=1 should be explained otherwise.

Lolli et al. (2009) found that high p and c values are estimated when fitting (by a MOM) sequences simulated according to a MSE or a LPL with an early onset of the exponential decay. We could argue that a similar phenomenon occurs in this case. We might say that, as c is not useful to reproduce the decay at short times because such times are excluded from computations, the MOM 'uses' c to reproduce the deviation of rate function from power law (due to the onset of the exponential decay). The better AICc and BIC scores of the MOM with respect to the MSE and the LPL can be explained as well by the fact that the latter models pay a penalty for a parameter (d for MSE and t_b for LPL) that is not useful to improve the fit at short times while the MOM can 'recycle' parameter c to improve the fit at long times. Hence we might consider the behavior

observed when *Ts*=1 as a further evidence of the emergence of the exponential decay for many sequences and of the inadequacy of the MOM to reproduce consistently their behavior.

When *Ts*=1 even the direct comparison between LPL and DRL (Table 5) shows significant variations with a reduction of the preferences to LPL for both AICc (2 sequences less) and BIC (4 sequences less). Conversely, the maximum log likelihood l_{max} of the LPL becomes the largest for all of the sequences. This means that the DRL is able to describe as well as the LPL the behavior at long times while it is less appropriate at short times where the earthquake catalog might be incomplete. We can argue that the DRL captures much of the true physical properties but it is not particularly suited in general to reproduce the empirical behavior of real sequences.

Conclusions

We verified that if background rate is modeled properly, the most of a set of 24 real sequences in Italy (6) and Southern California (18) show the emergence of a negative exponential decay of aftershock rate after the initial time interval where the power-law dominates. In fact, two decay models that predict such exponential decay – the Modified Stretched Exponential (MSE, Gross and Kisslinger, 1994) and the band Limited Power Law (LPL, Narteau et al, 2002) – have a higher maximum log-likelihood l_{max} than the Modified Omori Model (MOM, Utsu, 1971) for 23 sequences over 24. The MSE and the LPL are to be preferred with respect to the MOM for about one half of the sequences, on the basis of the corrected Akaike Information Criterion (AIC_c) and the Bayesian Information Criterion (*BIC*). In particular, the LPL alone performs better than the MOM for 18 sequences over 24 according to l_{max}, 14 to AIC_c and 10 to *BIC*. In most cases, the estimated characteristic times of the exponential decay are on the order of some weeks to some months.

The inclusion of the background in the rate equation is necessary because, when neglected, the emergence of the exponential decay is somehow hidden for many sequences. The inclusion of the background term has also the effect to reduce the estimates of the characteristic time of the

exponential decay (for the MSE and LPL) and to increase the estimates of the power-law exponent and, to a minor extent, of the initial delay time for all of the models and particularly for the MOM. As the LPL is generally preferable with respect to the MSE and is able to reproduce well the effective rate decay of real sequences in most cases, it is reasonable to adopt it (with background included) in future analyses of aftershock decay and particularly in real-time forecasts of aftershock probabilities (Gerstenberger et al., 2007) where the actual properties of the sequences are not known well.

We also found that an empirical rate formula equivalent to that predicted by the Dieterich (1994) rate- and state-dependent friction model, with only three free parameters, is able to explain quite well a significant portion of the sequences but performs generally worse than the LPL. This indicates that the Dieterich (1994) rate equation is able to describe well much of the physics of the process of aftershock generation but also that some further developments are needed to make it suitable for best reproducing the observed behavior of aftershock rates.

Acknowledgements

We thank an anonymous referee for some suggestions that were useful to strengthen the findings of the paper. This research has benefited from funding provided by the Italian Presidenza del Consiglio dei Ministri – Dipartimento della Protezione Civile (DPC). Scientific papers funded by DPC do not represent its official opinion and policies.

References

Akaike, H. (1974). A new look at the statistical model identification. IEEE Trans. On Automatic Control AC, 19, 716-723.

Castello, B., G., Selvaggi, C., Chiarabba, and A., Amato (2005). Catalogo della sismicità italiana – CSI 1.0 (1981-2002). Available at: http://www.ingv.it/CSI/.

CSTI Working Group (2004). Catalogo strumentale dei terremoti Italiani dal 1981 al 1996, Version 1.1, available at: http://ibogfs.df.unibo.it/user2/paolo/www/gndt/Versione1_1/Leggimi.htm.

Dennis, J.E., and R.B., Schnabel (1983). Numerical methods for unconstrained optimization and nonlinear equations. Prentice-Hall, Englewood Cliffs, New Jersey.

Dieterich, J. H. (1994). A constitutive law for rate of earthquake production and its application to earthquake clustering, J. Geophys. Res., 99, 2601-2618.

Draper, D. (1995). Assessment and propagation of model uncertainty (with discussion). J. Royal Stat. Soc., Series B, 57, 45-97.

Gardner, J.K., and L., Knopoff, (1974). Is the sequence of earthquakes in Southern California, with aftershocks removed, Poissonian? Bull. Seism. Soc. Am., 64, 1363-1367.

Gasperini, P., and B., Lolli, (2006). Correlation between the parameters of the aftershock rate equation: Implications for the forecasting of future sequences, Phys. Earth Plan. Int., 156, (41-58).

Gerstenberger, M.C., L.M., Jones and S., Wiemer (2007). Short-term Aftershock Probabilities: Case Studies in California, Seism. Res. Lett., 70, 66-77

Gross, S.J., and C., Kissilinger, (1994). Test of Models of aftershock rate decay. Bull. Seism. Soc. Am., 84, 1571-1579.

Hurvich, C.M., and C-L., Tsai (1989). Regression and time series model selection in small samples. Biometrika, 76, 297-307.

Kisslinger, C. (1993). The stretched exponential function as an alternative model for aftershock

427 decay rate. J. Geophys. Res., 98, 1913-1921.
428 Lolli, B., and P., Gasperini, (2003). Aftershocks hazard in Italy Part I: Estimation of time-
429 magnitude distribution model parameters and computation of probabilities of occurrence. J.
430 Seismol., 7, 235-257.
431 Lolli B., and P., Gasperini, (2006). Comparing different models of aftershock rate decay: The role
432 of catalog incompleteness in the first times after mainshock, Tectonophysics, 423, 43–59
433 Lolli B., E., Boschi, and P., Gasperini, (2009). A comparative analysis of different models of
434 aftershock rate decay by maximum likelihood estimation of simulated sequences, J. Geophys.
435 Res.,114, B01305, doi:10.1029/2008JB005614.
436 Nanjo, K. Z., B. Enescu, R. Shcherbatov, D. L. Turcotte, T. Iwata, and Y. Ogata (2007), Decay of
437 aftershock activity for Japanese earthquakes, J. Geophys. Res., 112, B08309,
438 doi:10.1029/2006JB004754.
439 Narteau, C., P., Shebalin, and M., Holschneider (2002). Temporal limits of the power law
440 aftershock decay rate. J. Geophys. Res., 107. (B12): art. no. 2359, doi:10.1029/2002JB001868.
441 Narteau, C., P., Shebalin, S., Hainzl, G., Zoller, and M., Holschneider, (2003). Emergence of a
442 band-limited power law in the aftershock decay rate of a slider-block model. Geophys Res.
443 Lett., 30 No. 11, art. No. 1568, doi:10.1029/2003GL017110.
444 Ogata, Y. (1988). Statistical models for earthquake occurrences and residual analysis for point
445 processes. J. Amer. Stat. Assoc., 83, 9-27.
446 Ouillon, G., and D. Sornette (2005). Magnitude-dependent Omori law: Theory and empirical study,
447 J. Geophys. Res., 110, B04306, doi:10.1029/2004JB003311.
448 Postpischl, D. (1985). Catalogo dei terremoti italiani dall'anno 1000 al 1980. Quaderni della
449 Ricerca Scientifica, 114 2B, CNR, Rome.
450 Schwarz, G. (1978). Estimating the dimension of a model. Annals of Statistics, 6, 461-464.
451 Utsu, T. (1961). A statistical study of the occurrence of aftershocks. Geophys. Mag. 30, 521-605.
452

Table captions

Table 1. List of sequences from Southern California (calxx) and Italy (itaxx) analyzed in this work. Dates and geographical coordinates refer to mainshock origin time and epicenter. M_m is the mainshock magnitude, $M_{\min}$ is the minimum magnitude of aftershocks, *Nev* is the number of aftershocks (above $M_{\min}$) within the influence zone of the mainshock, *D* is the effective duration of the sequence (the time difference between the mainshock and the last aftershock), and R_i the radius of the influence zone of the mainshock (see text).

Table 2. Parameters values and goodness-of-fit scores of the different decay models not including (left) and including (right) the background rate (μ, in shocks/day), for the maximum sequence duration of 48 months. p_1 is the power law exponent (p for the MOM, r for the MSE and q for the LPL), p_2 is the initial delay time (c for the MOM, d for the MSE, t_b for the LPL) in days, and p_3 the characteristic time of the negative exponential decay (not defined for the MOM, t_0 for the MSE, t_b for the LPL) in days. p_3 estimates definitely longer than the duration of the sequence (1460 days) are highlighted with bold type and those at the lower (1 day) and upper ($1 \quad 10^7$ days) limit assumed in maximum likelihood estimation are denoted by "Low lim." and "Up lim." respectively. AIC_c, BIC, and $l_{\max}$ are the goodness-of-fits scores for each decay model (without and with background). For each sequence, the higher score (highlighted with bold type) indicates the model preferred according to each criterion.

Table 3. Counts of sequences for which the different criteria assign the preference to various models, for the maximum sequence duration of 48 months.

Table 4. Parameters values and goodness-of-fit scores of the LPL (with background) and RDL decay models for a sequence duration of 48 months. p_1 is the power law exponent for the LPL, p_2 is

477 the initial delay time (t_b for the LPL, Ct_c for the DRL) in days, and p_3 the characteristic time of the
478 negative exponential decay (t_b for the LPL and t_c for the DRL) in days. p_3 estimates definitely
479 longer than the duration of the sequence (1460 days) are highlighted with bold type and those at the
480 lower (1 day) and upper (1 10^7 days) limit are denoted by "Low lim." and "Up lim." respectively.
481 AIC_c, BIC, and l_{max} are the goodness-of-fits scores for each decay model. For each sequence, the
482 higher score (highlighted with bold type) indicates the model preferred according to each criterion.
483
484 Table 5. Counts of sequences, from California and Italy, for which the different criteria assign the
485 preference to various models, for the maximum sequence duration of 48 months and different
486 starting times T_s (in days) of the observing time interval.
487
488 Table 6. Parameters values of the MOM for different starting times T_s (in days) of the observing
489 time interval. Values of p>1.5 and c>1 day are highlighted with bold type.
490

490 **Table 1**

491 **Detected sequences**

Seq.	Year	Mo	Day	Lat (North)	Lon (East)	M_m	M_{min}	Nev	D (days)	R_i (km)
cal01	1933	3	11	33.638	-117.973	6.4	3.0	269	1451	42
cal02	1946	3	15	35.702	-117.944	6.3	3.0	154	1364	30
cal03	1947	4	10	34.983	-116.531	6.5	3.0	124	1455	27
cal04	1954	3	19	33.298	-116.081	6.4	3.0	136	1452	32
cal05	1968	4	9	33.167	-116.087	6.6	3.1	162	1445	52
cal06	1971	2	9	34.416	-118.370	6.6	3.1	291	1408	27
cal07	1979	3	15	34.327	-116.445	5.3	2.5	176	1451	13
cal08	1981	4	26	33.096	-115.624	5.8	2.5	186	1425	16
cal09	1986	7	8	33.999	-116.608	5.7	2.5	868	1452	44
cal10	1986	7	13	32.971	-117.874	5.5	2.5	1686	1457	22
cal11	1987	2	7	32.388	-115.305	5.4	2.5	225	1454	40
cal12	1987	11	24	33.015	-115.852	6.6	3.1	216	1446	41
cal13	1994	1	17	34.213	-118.537	6.7	3.2	344	1455	25
cal14	1999	10	16	34.594	-116.271	7.1	3.6	151	1367	52
cal15	2001	7	17	36.016	-117.874	5.2	1.7	2009	1457	28
cal16	2002	2	22	32.319	-115.322	5.7	2.2	785	1457	27
cal17	2003	12	22	35.709	-121.104	6.5	3.0	129	1444	32
cal18	2004	9	28	35.812	-120.379	6.0	2.5	147	1377	48
ita01	1980	11	23	40.800	15.367	6.5	3.0	105	1407	41
ita02	1984	4	29	43.204	12.585	5.2	2.5	130	1459	41
ita03	1990	5	5	40.650	15.882	5.6	2.5	109	1453	41
ita04	1997	9	26	43.015	12.854	5.8	2.5	774	1354	46
ita05	2002	9	6	38.381	13.654	5.6	2.5	181	1414	26
ita06	2002	10	31	41.717	14.893	5.4	2.5	163	1280	26

492

Table 2

Parameters values and goodness-of-fit scores

Seq.	Model	Without background						With background						
		p1	p2	p3	AICc	BIC		μ	p1	p2	p3	AICc	BIC	
cal01	MOM	1.090	0.061		210.778	208.188	213.823	0.012	1.160	0.082		211.467	208.029	215.542
	MSE	0.886	0.029	Low Lim.	206.087	202.649	210.163	0.011	0.837	0.030	Low Lim.	205.811	201.533	210.926
	LPL	1.080	0.055	**Up. Lim.**	**211.975**	**208.538**	**216.051**	0.011	1.130	0.073	**9.1E+06**	**212.352**	**208.074**	**217.467**
cal02	MOM	1.180	1.360		-139.495	-141.213	-136.415	0.008	1.290	1.780		-139.746	-142.010	-135.611
	MSE	0.847	0.861	Low Lim.	-142.022	-144.286	-137.888	0.010	0.795	1.030	Low Lim.	-142.147	-144.942	-136.944
	LPL	1.130	0.868	**Up. Lim.**	**-137.854**	**-140.118**	**-133.720**	0.006	1.190	1.150	**5.8E+06**	**-138.479**	**-141.274**	**-133.276**
cal03	MOM	0.974	0.008		**-37.758**	**-39.132**	**-34.658**	0.004	1.000	0.012		**-38.578**	**-40.374**	-34.409
	MSE	0.948	0.008	**Up. Lim.**	-38.828	-40.624	-34.660	0.011	0.797	0.003	5	-39.249	-41.451	**-33.995**
	LPL	0.955	0.005	**8.7E6**	-39.322	-41.119	-35.154	0.014	0.933	0.004	373	-40.007	-42.209	-34.753
cal04	MOM	1.050	0.005		**116.559**	**115.038**	119.650	0.010	1.130	0.010		119.506	117.509	123.659
	MSE	0.950	0.003	Low Lim.	114.436	112.439	118.588	0.014	0.742	0.001	Low Lim.	119.142	116.686	124.373
	LPL	1.040	0.005	**Up. Lim.**	115.787	113.790	**119.939**	0.016	1.010	0.005	94	**121.385**	**118.928**	**126.615**
cal05	MOM	0.850	0.008		**-212.914**	**-214.713**	-209.838	0.045	1.210	0.108		**-196.063**	**-198.435**	-191.935
	MSE	0.831	0.007	**Up. Lim.**	-214.668	-217.040	-210.541	0.051	0.725	0.031	Low Lim.	-196.443	-199.375	**-191.251**
	LPL	0.849	0.011	**Up. Lim.**	-213.667	-216.040	**-209.540**	0.052	0.979	0.036	59	-196.518	-199.450	-191.326
cal06	MOM	1.050	0.002		**650.169**	**647.457**	**653.210**	0.003	1.060	0.002		649.272	**645.671**	653.342
	MSE	0.872	0.001	Low Lim.	648.102	644.501	652.172	0.013	0.807	0.001	Low Lim.	648.499	644.015	653.604
	LPL	1.030	0.001	**Up. Lim.**	648.319	644.718	652.389	0.022	0.992	0.001	190	**650.093**	645.609	**655.198**
cal07	MOM	0.983	0.042		**-79.017**	**-80.946**	-75.947	0.002	0.993	0.046		**-80.042**	**-82.590**	-75.925
	MSE	0.869	0.026	102	-79.962	-82.511	**-75.845**	0.017	0.697	0.002	12	-80.096	-83.251	**-74.920**
	LPL	0.973	0.040	**Up. Lim.**	-80.996	-83.544	-76.879	0.025	0.799	3.4E-07	104	-81.636	-84.791	-76.459
cal08	MOM	1.080	0.018		134.924	132.908	137.990	0.036	1.860	0.229		187.611	**184.946**	191.722
	MSE	0.999	0.003	Low Lim.	130.356	127.690	134.466	0.036	0.501	1.0E-06	Low Lim.	175.349	172.046	180.516
	LPL	1.090	0.028	**Up. Lim.**	**136.149**	**133.483**	**140.259**	0.036	1.540	0.139	46	**187.865**	184.562	**193.031**
cal09	MOM	0.802	0.002		**100.959**	**96.580**	103.973	0.253	1.070	0.035		**171.333**	**165.500**	175.357
	MSE	0.788	0.001	**Up. Lim.**	96.460	90.626	100.483	0.280	0.809	0.018	Low Lim.	170.929	163.643	**175.964**
	LPL	0.803	0.003	**Up. Lim.**	100.924	95.090	**104.947**	0.274	1.030	0.024	773	168.214	160.928	173.249

Table 2 (continued)

Seq.	Model	Without background						With background						
		p1	p2	p3	AICc	BIC		μ,M	p1	p2	p3	AICc	BIC	
cal10	MOM	0.725	0.031		183.112	177.731	186.119	1.2E-05	0.725	0.031		182.106	174.934	186.118
	MSE	0.598	1.0E-06	1260	193.267	186.095	197.279	1.2E-05	0.598	1.0E-06	1260	192.261	183.298	197.279
	LPL	0.630	4.1E-06	**1790**	**194.930**	**187.757**	**198.942**	1.2E-05	0.630	3.2E-06	**1790**	**193.924**	**184.961**	**198.942**
cal11	MOM	0.673	1.0E-06		**-465.255**	**-467.568**	**-462.200**	0.116	1.570	0.163		-431.516	**-434.581**	-427.425
	MSE	0.664	1.0E-06	**Up. Lim.**	-466.999	-470.064	-462.908	0.118	0.464	1.0E-06	Low Lim.	-432.487	-436.296	-427.350
	LPL	0.673	3.2E-05	**Up. Lim.**	-466.347	-469.413	-462.256	0.119	0.626	3.4E-06	2	**-431.204**	-435.012	**-426.067**
cal12	MOM	0.962	0.009		15.087	**12.837**	18.143	0.055	1.450	0.090		**44.980**	**42.000**	**49.075**
	MSE	0.945	0.010	**Up. Lim.**	13.480	10.500	17.575	0.060	0.552	0.001	Low Lim.	38.095	34.394	43.238
	LPL	0.961	0.011	**Up. Lim.**	**15.495**	12.515	**19.590**	0.053	1.340	0.064	**4.0E+06**	43.005	39.305	48.148
cal13	MOM	1.150	0.066		**529.989**	**527.020**	**533.024**	0.016	1.260	0.110		533.566	529.620	537.625
	MSE	0.838	0.020	1	523.966	520.019	528.025	0.027	0.723	0.020	Low Lim.	**535.597**	**530.679**	**540.686**
	LPL	1.130	0.051	**Up. Lim.**	525.881	521.934	529.940	0.027	1.110	0.054	197	530.123	525.205	535.212
cal14	MOM	1.190	0.037		**206.291**	**204.603**	**209.372**	0.002	1.220	0.045		205.622	203.401	209.759
	MSE	0.794	0.005	1	204.637	202.415	208.774	0.008	0.703	0.003	Low Lim.	**209.143**	**206.401**	**214.349**
	LPL	1.150	0.025	**Up. Lim.**	203.749	201.527	207.886	0.010	0.945	0.008	40	206.945	204.203	212.152
cal15	MOM	0.951	0.165		**2646.788**	**2641.143**	**2649.794**	0.297	1.290	1.070		2702.098	2694.573	2706.108
	MSE	0.922	0.160	**Up. Lim.**	2645.082	2637.557	2649.092	0.411	0.462	1.0E-06	12	2782.900	2773.496	2787.915
	LPL	0.925	0.110	**Up. Lim.**	2634.159	2626.634	2638.169	0.423	0.547	0.002	26	**2783.754**	**2774.350**	**2788.768**
cal16	MOM	0.745	0.003		**-365.589**	**-369.816**	-362.574	0.308	1.740	1.150		-194.518	-200.148	-190.492
	MSE	0.732	0.002	**Up. Lim.**	-370.059	-375.689	-366.033	0.313	0.624	0.240	Low Lim.	-188.049	-195.080	-183.010
	LPL	0.746	0.008	**Up. Lim.**	-366.548	-372.178	**-362.523**	0.317	0.489	8.5E-07	6	**-184.342**	**-191.373**	**-179.303**
cal17	MOM	0.994	0.025		**-86.333**	**-87.770**	-83.237	0.002	1.010	0.033		**-87.325**	**-89.208**	-83.164
	MSE	0.895	0.014	55	-87.350	-89.233	**-83.189**	0.012	0.745	1.0E-06	7	-87.635	-89.946	**-82.391**
	LPL	0.976	0.018	**Up. Lim.**	-87.793	-89.676	-83.632	0.016	0.919	6.2E-06	253	-88.705	-91.016	-83.461
cal18	MOM	0.645	1.0E-06		**-377.158**	**-378.803**	**-374.074**	0.057	0.865	1.0E-06		**-368.524**	**-370.688**	-364.383
	MSE	0.639	1.0E-06	**Up. Lim.**	-378.495	-380.659	-374.354	0.057	0.850	1.0E-06	**Up Lim.**	-369.634	-372.302	-364.421
	LPL	0.645	1.4E-06	**Up. Lim.**	-378.249	-380.414	-374.109	0.065	0.856	2.8E-06	711	-369.560	-372.229	**-364.347**

Table 2 (continued)

Seq.	Model	Without background						With background						
		p1	p2	p3	AICc	BIC		μ	p1	p2	p3	AICc	BIC	
ita01	MOM	0.861	0.038		**-202.562**	**-203.668**	-199.444	7.5E-07	0.861	0.038		**-203.644**	**-205.076**	-199.444
	MSE	0.745	0.005	1260	-203.462	-204.895	**-199.262**	0.012	0.654	1.0E-06	60	-204.180	-205.917	-198.877
	LPL	0.829	0.026	**6810**	-203.817	-205.249	-199.617	0.019	0.730	7.5E-06	194	-204.178	-205.915	**-198.875**
ita02	MOM	0.908	0.005		**-127.406**	**-128.856**	**-124.311**	0.025	1.210	0.122		-120.859	-122.758	-116.699
	MSE	0.883	0.004	**Up. Lim.**	-128.684	-130.583	-124.524	0.032	0.559	1.0E-06	3	-115.481	-117.813	-110.239
	LPL	0.890	1.3E-07	**Up. Lim.**	-128.714	-130.614	-124.554	0.032	0.730	2.3E-06	19	**-115.416**	**-117.748**	**-110.174**
ita03	MOM	0.771	1.0E-06		**-243.151**	**-244.317**	**-240.037**	0.034	0.987	0.007		**-236.613**	**-238.127**	-232.420
	MSE	0.759	1.0E-06	**Up. Lim.**	-244.665	-246.180	-240.473	0.045	0.671	1.0E-06	2	-237.386	-239.228	-232.095
	LPL	0.771	8.1E-07	**Up. Lim.**	-244.237	-245.752	-240.045	0.047	0.753	4.6E-06	10	-237.106	-238.949	**-231.815**
ita04	MOM	1.340	4.050		497.048	492.843	500.064	5.8E-06	1.340	4.050		496.038	490.436	500.064
	MSE	0.572	0.048	42	**511.769**	**506.167**	**515.795**	0.046	0.455	1.0E-06	31	**526.315**	**519.320**	**531.354**
	LPL	0.750	0.083	330	491.742	486.141	495.768	0.050	0.551	0.008	71	523.765	516.770	528.804
ita05	MOM	0.960	0.061		-126.564	-128.537	-123.496	1.3E-06	0.960	0.061		-127.610	-130.218	-123.496
	MSE	0.720	0.007	70	**-124.837**	**-127.444**	**-120.723**	0.023	0.515	1.0E-06	15	-115.103	-118.333	-109.931
	LPL	0.899	0.026	**3430**	-128.744	-131.352	-124.631	0.025	0.623	1.2E-06	48	**-112.481**	**-115.712**	**-107.310**
ita06	MOM	0.974	0.331		-199.462	**-201.270**	-196.386	0.019	1.110	0.587		-199.809	**-202.195**	-195.683
	MSE	0.951	0.338	**Up. Lim.**	-200.571	-202.956	-196.444	0.007	0.998	0.356	2	-201.228	-204.177	-196.037
	LPL	0.974	0.358	**Up. Lim.**	**-199.165**	-201.551	**-195.039**	0.019	1.090	0.508	**6.1E+06**	**-199.329**	-202.278	**-194.138**

499 **Table 3**

500 **Counts of preferred models (including background)**

	California			Italy			California+Italy		
Model	AICc	BIC		AICc	BIC		AICc	BIC	
MOM	7	10	1	2	3	0	9	13	1
MSE	2	2	7	1	1	1	3	3	8
LPL	9	6	10	3	2	5	12	8	15
MOM	8	11	6	2	3	0	10	14	6
LPL	10	7	12	4	3	6	14	10	18
MOM	13	13	5	3	3	1	16	16	6
MSE	5	5	13	3	3	5	8	8	18
MSE		7			1			8	
LPL		11			5			16	
LPL	14	13	14	3	3	6	17	16	20
DRL	4	5	4	3	3	0	7	8	4

501

502

502 **Table 4**

503 **Parameters values and goodness-of-fit scores**

Seq.	Model	μ	p1	p2	p3	AICc	BIC	
cal01	LPL	0.011	1.130	0.073	**9.1E+06**	**212.352**	**208.074**	**217.467**
	DRL	1.0E-07		0.025	**2.4E+08**	205.206	202.616	208.251
cal02	LPL	0.006	1.190	1.150	**5.8E+06**	**-138.479**	**-141.274**	**-133.276**
	DRL	4.5E-09		0.545	**4.4E+09**	-144.569	-146.288	-141.489
cal03	LPL	0.014	0.933	0.004	373	-40.007	-42.209	-34.753
	DRL	0.007		0.011	**1390**	**-37.499**	**-38.872**	**-34.399**
cal04	LPL	0.016	1.010	0.005	94	**121.385**	**118.928**	**126.615**
	DRL	0.008		0.002	1340	116.246	114.725	119.337
cal05	LPL	0.052	0.979	0.036	59	**-196.518**	-199.450	**-191.326**
	DRL	0.047		0.029	223	-196.811	**-198.610**	-193.735
cal06	LPL	0.022	0.992	0.001	190	**650.093**	**645.609**	**655.198**
	DRL	2.0E-06		0.001	**1.1E+07**	646.748	644.036	649.789
cal07	LPL	0.025	0.799	3.4E-07	104	-81.636	-84.791	-76.459
	DRL	0.004		0.050	**3890**	**-79.000**	**-80.929**	**-75.930**
cal08	LPL	0.036	1.540	0.139	46	**187.865**	**184.562**	**193.031**
	DRL	0.030		4.5E-08	454	140.317	138.301	143.383
cal09	LPL	0.274	1.030	0.024	773	168.214	160.928	173.249
	DRL	0.290		0.021	173	**170.673**	**166.294**	**173.687**
cal10	LPL	1.2E-05	0.630	3.2E-06	**1790**	**193.924**	**184.961**	**198.942**
	DRL	0.346		1.760	597	115.124	109.743	118.131
cal11	LPL	0.119	0.626	3.4E-06	2	**-431.204**	**-435.012**	**-426.067**
	DRL	0.114		0.007	61	-434.675	-436.988	-431.621
cal12	LPL	0.053	1.340	0.064	**4.0E+06**	**43.005**	**39.305**	**48.148**
	DRL	0.043		0.009	346	28.513	26.263	31.569
cal13	LPL	0.027	1.110	0.054	197	**530.123**	**525.205**	**535.212**
	DRL	1.9E-07		0.016	**1.6E+08**	514.042	511.073	517.077
cal14	LPL	0.010	0.945	0.008	40	**206.945**	**204.203**	**212.152**
	DRL	3.1E-07		0.004	**4.1E+07**	194.681	192.993	197.762
cal15	LPL	0.423	0.547	0.002	26	**2783.754**	**2774.350**	**2788.768**
	DRL	0.265		0.200	761	2681.258	2675.612	2684.264
cal16	LPL	0.317	0.489	8.5E-07	6	**-184.342**	**-191.373**	**-179.303**
	DRL	0.307		0.077	147	-219.133	-223.360	-216.118
cal17	LPL	0.016	0.919	6.2E-06	253	-88.705	-91.016	-83.461
	DRL	0.003		0.026	**4530**	**-86.282**	**-87.719**	**-83.186**
cal18	LPL	0.065	0.856	2.8E-06	711	**-369.560**	**-372.229**	**-364.347**
	DRL	0.075		0.013	70	-371.459	-373.104	-368.375

504

504 **Table 4 (continued)**

505

Seq.	Model	μ	p1	p2	p3	AICc	BIC	
ita01	LPL	0.019	0.730	7.5E-06	194	-204.178	-205.915	**-198.875**
	DRL	0.014		0.223	751	**-203.952**	**-205.058**	-200.833
ita02	LPL	0.032	0.730	2.3E-06	19	**-115.416**	**-117.748**	**-110.174**
	DRL	0.026		0.019	370	-121.550	-122.999	-118.455
ita03	LPL	0.047	0.753	4.6E-06	10	-237.106	-238.949	**-231.815**
	DRL	0.043		0.009	121	**-236.343**	**-237.509**	-233.229
ita04	LPL	0.050	0.551	0.008	71	**523.765**	**516.770**	**528.804**
	DRL	2.2E-08		0.517	**4.4E+09**	467.306	463.101	470.322
ita05	LPL	0.025	0.623	1.2E-06	48	**-112.481**	**-115.712**	**-107.310**
	DRL	0.007		0.097	**2820**	-126.766	-128.739	-123.698
ita06	LPL	0.019	1.090	0.508	**6.1E+06**	-199.329	-202.278	**-194.138**
	DRL	0.011		0.365	**1760**	**-199.197**	**-201.005**	-196.121

506

507

507 **Table 5**

508 **Counts of preferred models using different starting times T_s**

509

	T_s=t_1			T_s =0.007			T_s =0.042			T_s =1		
Model	AICc	BIC		AICc	BIC		AICc	BIC		AICc	BIC	
MOM	9	13	1	10	13	1	11	14	2	20	21	4
MSE	3	3	8	4	3	8	3	3	4	0	0	2
LPL	12	8	15	10	8	15	10	7	18	4	3	18
LPL	17	16	20	17	16	22	18	16	22	15	12	24
DRL	7	8	4	7	8	2	6	8	2	9	12	0

510

511

511 **Table 6**

512 **MOM parameter estimates using different starting times T_s**

513

	$T_s = t_1$			$T_s = 1$		
Seq.	μ	p	c	μ	p	c
cal01	0.012	1.160	0.082	0.003	1.030	0.000
cal02	0.008	1.290	**1.780**	0.005	1.170	0.100
cal03	0.004	1.000	0.012	0.005	0.988	0.006
cal04	0.010	1.130	0.010	0.015	**2.130**	**9.890**
cal05	0.045	1.210	0.108	0.049	1.450	**1.140**
cal06	0.003	1.060	0.002	0.013	1.340	**2.350**
cal07	0.002	0.993	0.046	0.009	1.140	**1.190**
cal08	0.036	**1.860**	0.229	0.036	**1.750**	0.000
cal09	0.253	1.070	0.035	0.273	1.220	0.830
cal10	0.000	0.725	0.031	0.000	0.817	**2.790**
cal11	0.116	**1.570**	0.163	0.119	**4.000**	**5.120**
cal12	0.055	1.450	0.090	0.056	1.500	0.000
cal13	0.016	1.260	0.110	0.020	1.330	0.000
cal14	0.002	1.220	0.045	0.007	**1.780**	**2.000**
cal15	0.297	1.290	**1.070**	0.395	**2.180**	**12.600**
cal16	0.308	**1.740**	**1.150**	0.315	**3.130**	**9.170**
cal17	0.002	1.010	0.033	0.011	1.290	**1.450**
cal18	0.057	0.865	0.000	0.055	0.906	1.680
ita01	0.000	0.861	0.038	0.004	0.942	0.370
ita02	0.025	1.210	0.122	0.032	**2.400**	**6.090**
ita03	0.034	0.987	0.007	0.043	1.330	0.000
ita04	0.000	1.340	**4.050**	0.032	**1.870**	**18.600**
ita05	0.000	0.960	0.061	0.024	**2.790**	**31.000**
ita06	0.019	1.110	0.587	0.029	1.210	0.000

514

Figure captions

Figure 1. Number of sequences of Southern California for which each decay model is preferable according to AIC_c (a), *BIC* (b) and maximum log-likelihood (c) as a function of the duration of the sequence, when the background rate is neglected.

Figure 2. Number of sequences of Southern California for which each decay model is preferable according to AIC_c (a), *BIC* (b) and maximum log-likelihood (c) as a function of the duration of the sequence, when the background rate is modeled.

Figure 3. Number of sequences of Italy for which each decay model is preferable according to AIC_c as a function of the duration of the sequence, when the background rate is neglected (a) or modeled (b).

Figure 4. Number of sequences of Italy and Souther California for which the LPL (with background) or the DRL models are preferable according to AIC_c (a) or *BIC* (b) and maximum log-likelihood (c) as a function of the duration of the sequence.

Figure 5. Observed (symbols) and predicted (lines) aftershock rates as a function of time elapsed after the mainshock when the background rate is modeled for two sequences showing the clear emergence of the exponential decay at relatively long times.

Figure 6. Differences between observed and predicted cumulative number of aftershocks as a function of time elapsed after the mainshock for the same two sequences of Fig. 5.

539 Figure 7. Observed (symbols) and predicted (lines) aftershock rates (a), and differences between
540 observed and predicted cumulative number of aftershocks (b) as a function of time elapsed after the
541 mainshock when the background rate is modeled, for a sequence characterized by an high power
542 law exponent (p=1.86 for the MOM and q=1.54 for the LPL).
543

543 **Figure 1**

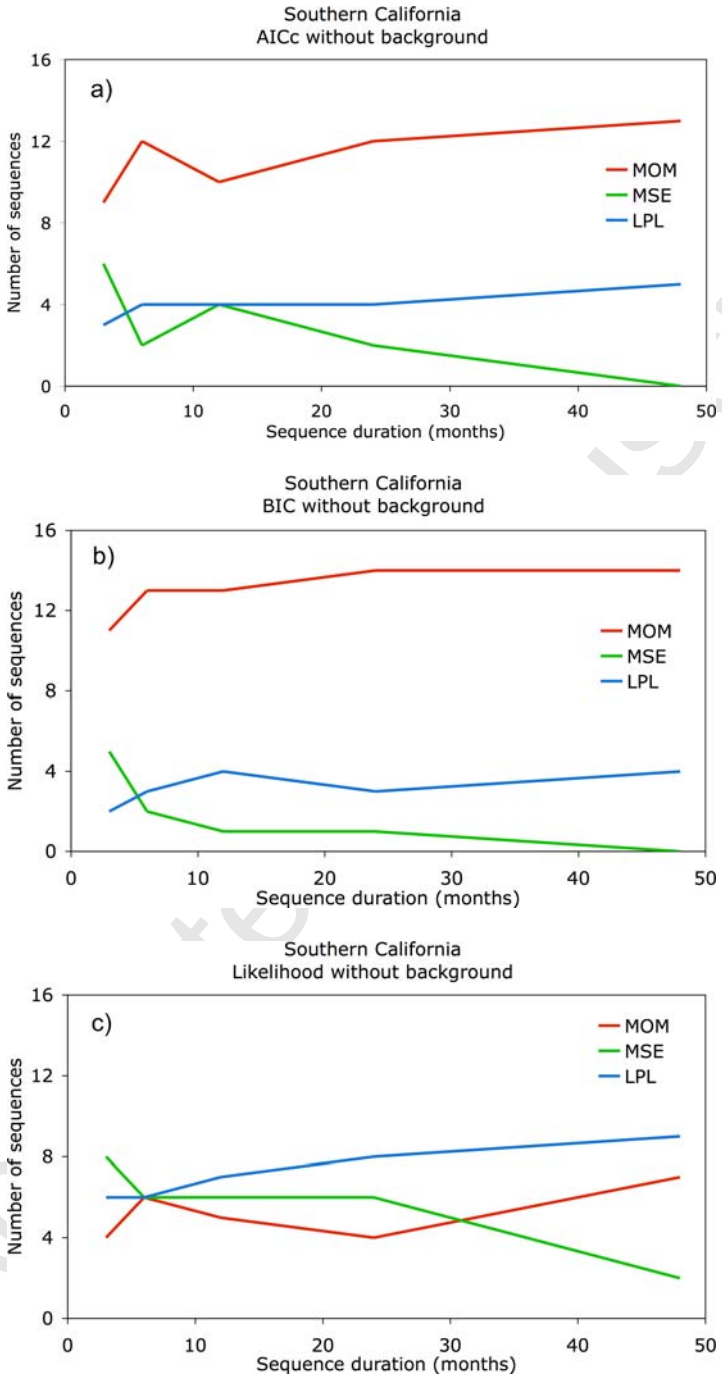

544

545

546

547

547 **Figure 2**

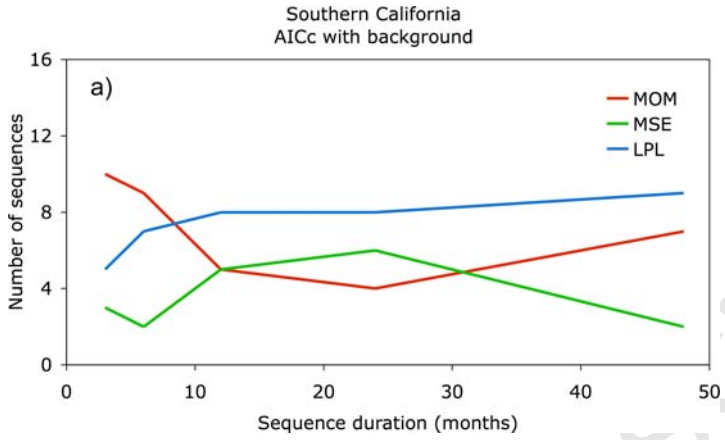

548

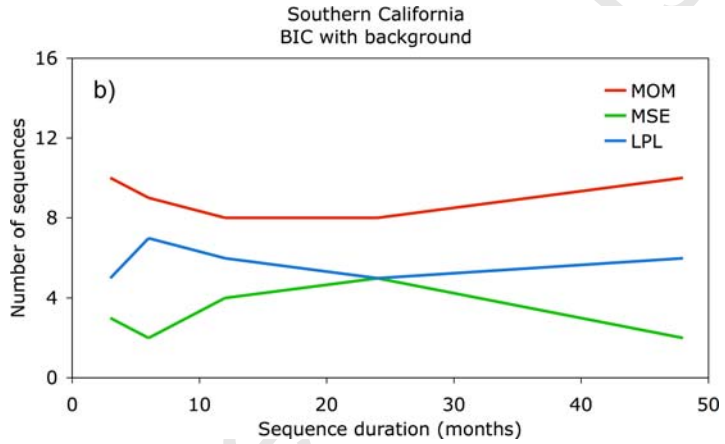

549

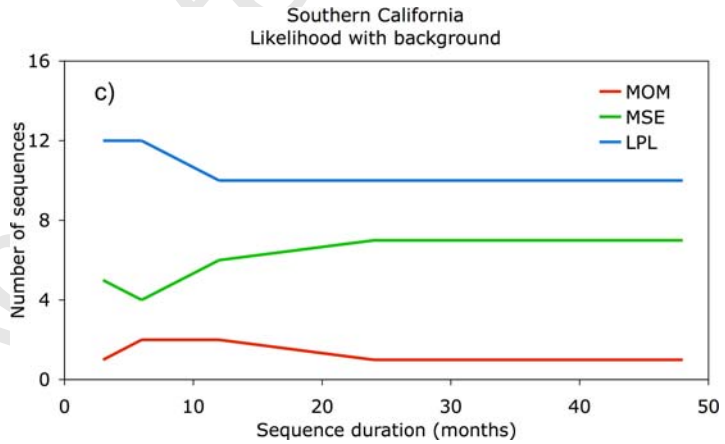

550

551

551 **Figure 3**

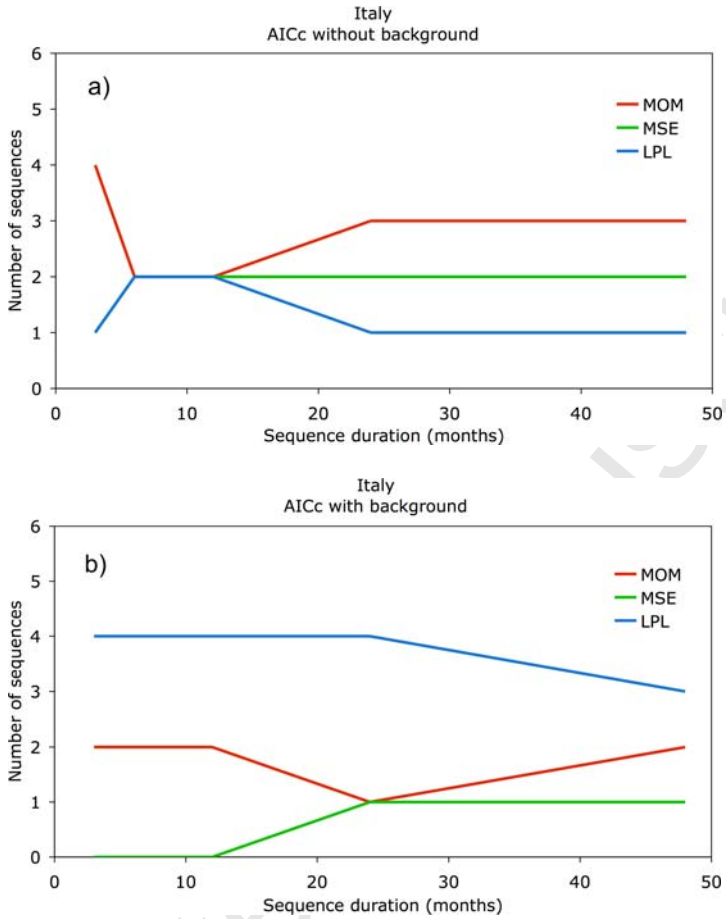

552

553

554

554 **Figure 4**

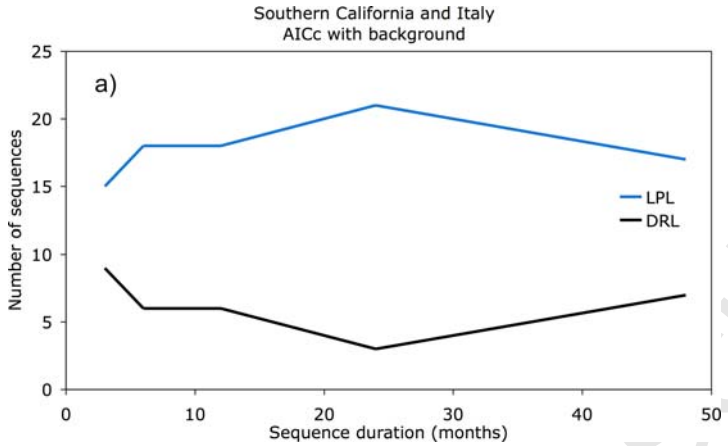

555

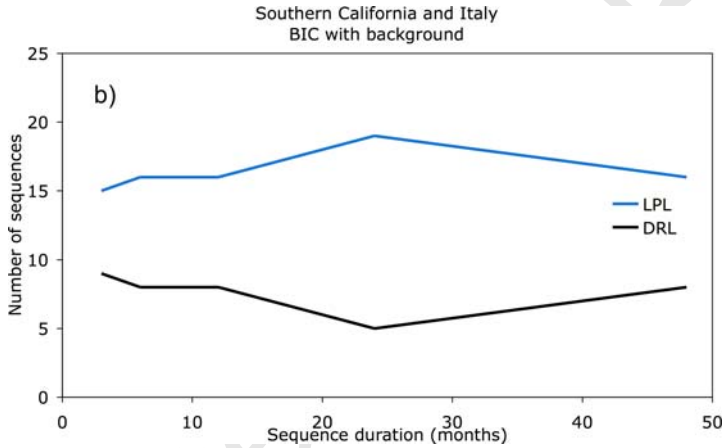

556

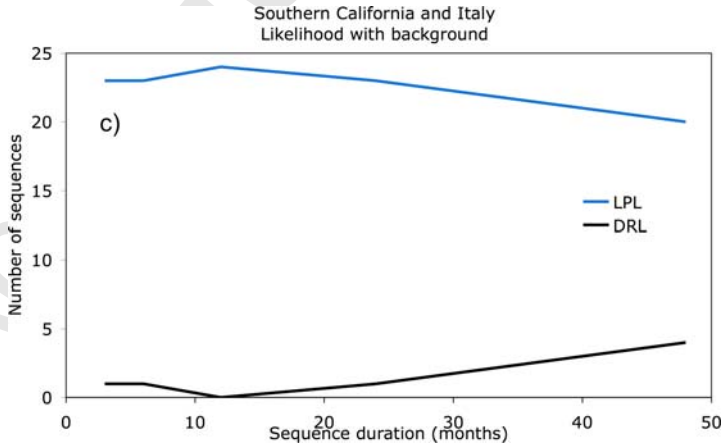

557

558 **Figure 5**

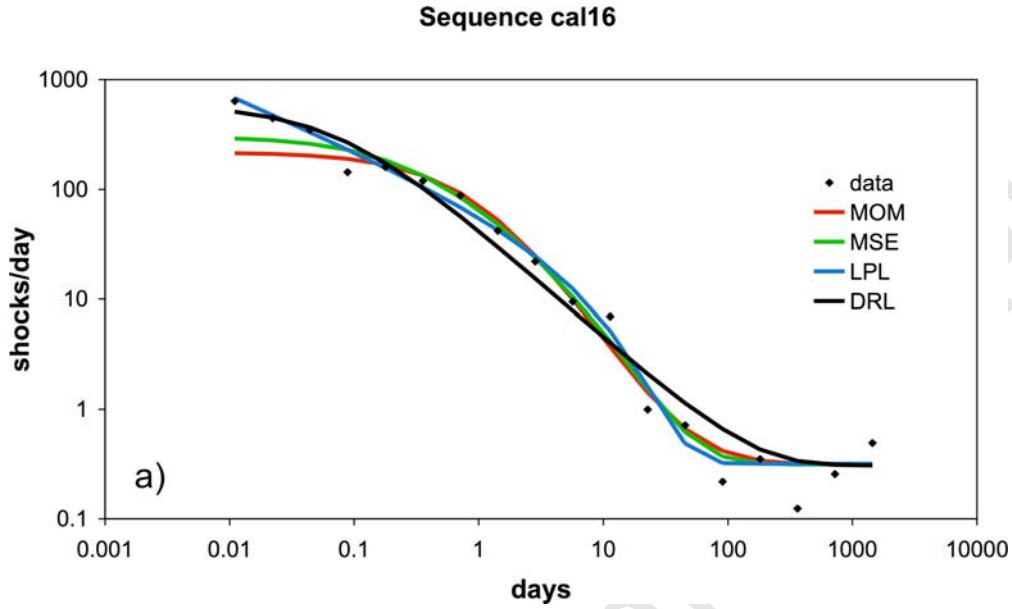

559

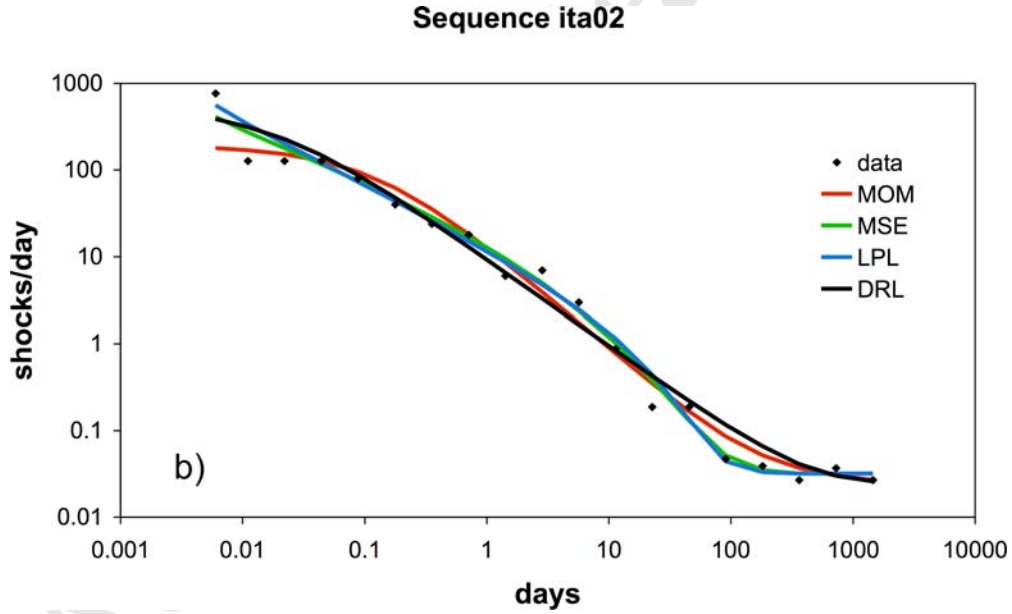

560

561

561 **Figure 6**

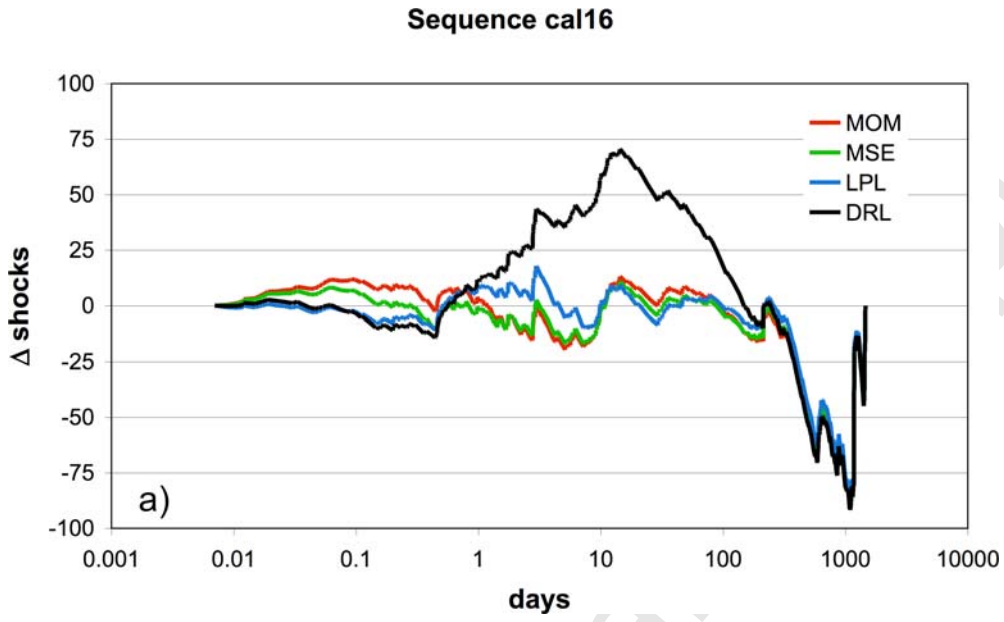

562

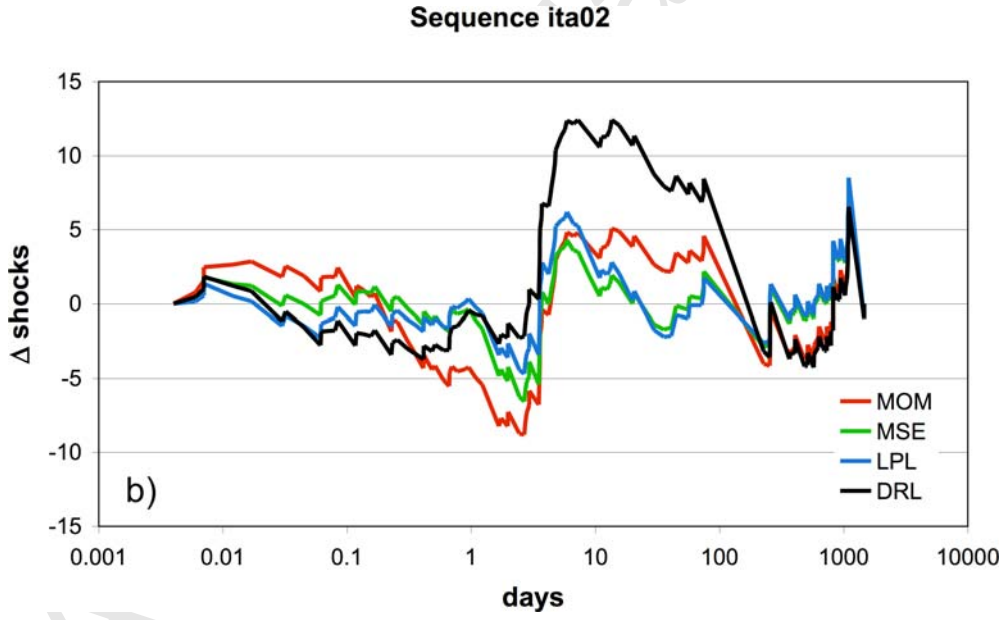

563

564 **Figure 7**

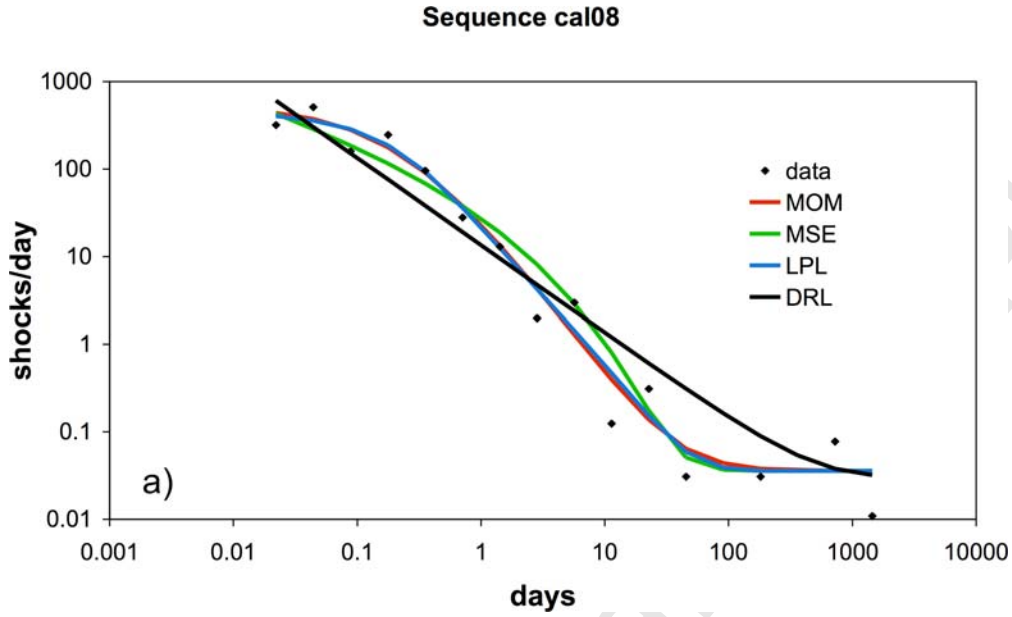

565

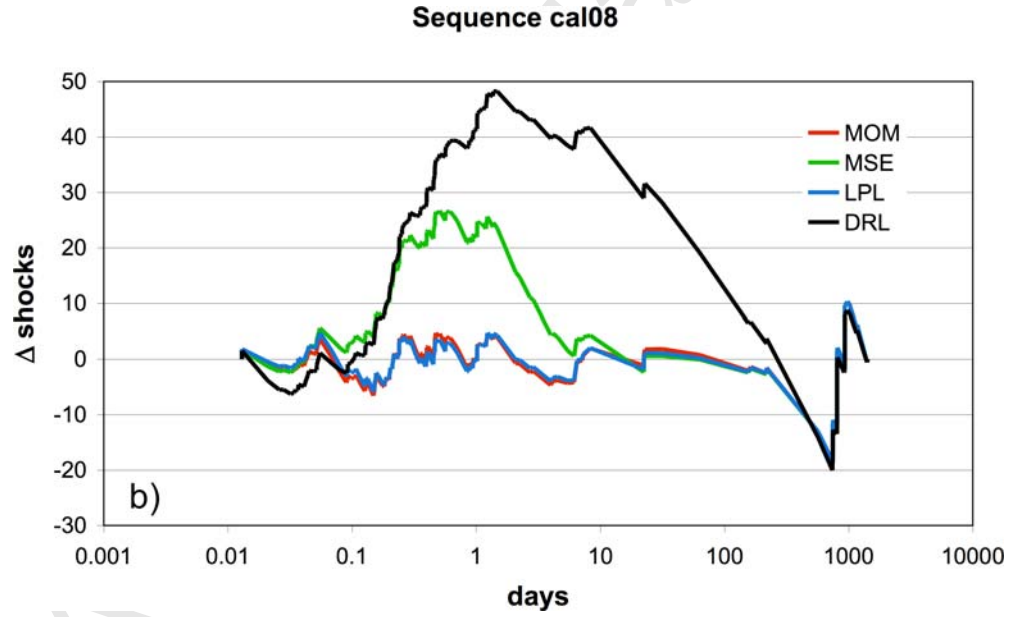

566